

Mechanisms, Kinetics and Thermodynamics of Mechanical Alloying in Immiscible Fe–Mg System

E. P. YELSUKOV, G. A. DOROFEEV, A. L. ULYANOV and A. N. MARATKANOVA

*Physical-technical Institute, Ural Branch of the Russian Academy of Sciences,
Ul. Kirova 132, Izhevsk 426001 (Russia)*

E-mail: Yelsukov@fnms.fti.udm.ru

Abstract

The processes involved in mechanical alloying (MA) of the mixture of Fe and Mg non-dissolving in equilibrium at the atomic ratio of 93 : 7 are studied by means of X-ray diffraction, Mossbauer spectroscopy, Auger electron and secondary ion mass spectrometry, chemical analysis of the composition. Surface enrichment of the powder particles with magnesium is observed at the first stage of MA. It is concluded that Mg gets segregated not only on the surface of particles but also within α -Fe grains. With a decrease in crystallite size (to ~ 10 nm), supersaturated solid solution of Mg in α -Fe is formed in the particles of the latter component, which is observed as an increase (to 0.288 nm) in the parameter of the bcc lattice and the appearance of additional components in the Mossbauer spectrum. It was established on the basis of model thermodynamic calculations that the driving force of the formation of solid solution in the system Fe–Mg may be the accumulated excess energy of coherent interphase boundaries of the Fe/Mg nanocomposite formed at the initial step of MA.

INTRODUCTION

Investigations of solid-phase reactions (SPR) that occur during mechanical alloying (MA) of iron with sp elements (C, Si, Ge and Sn) showed [1–6] that the necessary condition for these reactions to proceed is the achievement of nano-structured state in the components of a mixture under grinding, independently of the types of diagrams of state of the indicated binary systems. The final phase state in these systems (ferric carbide in Fe–C system or supersaturated solid solution (SSS) in the systems containing Fe with Si, Ge or Sn) arises through the formation of intermediate intermetallides or amorphous phases based on them. The multistage character of MA is likely to be connected with thermodynamics of alloys, namely, with the negative energy of component mixing in these systems and, as a consequence, with the presence of stable intermetallic compounds.

In order to reveal the regularities of SPR, it seems interesting to investigate MA in powder mixtures of the components immiscible at

equilibrium, that is, the components with the positive energy of mixing. These systems of the kind of iron – an sp element include a mixture of iron with magnesium. In the free state, the configuration of the outer electron shell of Mg atom is $3s^2p^0$. The solubility of Mg in Fe and Fe in Mg in the solid state is absent; the phase diagram does not contain any chemical compounds and intermediate phases [7]. The atomic radii of Fe and Mg, both metal (0.124 and 0.160 nm) and covalent ones (0.117 and 0.130 nm, respectively) differ substantially from each other. When investigating the structural and phase state of mixtures of Fe and Mg powders ground for a long time, the authors of [8] were the first to show the possibility to obtain SSS of Mg in Fe with the atomic concentration of Mg in the initial mixture not higher than 18 %. For different compositions, the system remained almost completely immiscible. In our studies [9], the maximal mass concentration of Mg in the SSS α -Fe(Mg) was 5–7 % and was observed only during MA of the mixture the composition of which was close to this saturation limit. An increase in the atomic concentra-

tion of Mg in the initial mixture to >10–15 % caused the absence of miscibility of the larger part of magnesium, that is, the formation of a two-phase mixture α -Fe(Mg) + HCP Mg with a decrease in the concentration of Mg in the formed SSS. It was established with the help of thermodynamic calculations [9] that the driving force of the formation of solid solution can be the accumulated energy of coherent inter-phase boundaries in Fe/Mg nanocomposite in which magnesium is epitaxially bound with the bcc structure of α -Fe. However, the absence of any data on the kinetics of atomic mixing for the composition for which a complete dissolution of the component occurs does not allow us to consider the mechanisms of MA in Fe–Mg system in detail.

The goal of the present work was to investigate the mechanisms, kinetics and thermodynamic driving forces of MA in Fe–Mg system with the initial atomic concentration of Mg in the mixture equal to 7 %.

EXPERIMENTAL

A mixture of iron powder (concentration of Fe: 99.98 mass %) and magnesium powder (concentration of Mg: 99.9 mass %) with the particle size less than 300 m was used for MA. Mechanical alloying was carried out in inert environment (Ar) in a ball planetary mill Fritsch P-7 with power intensity of 2.0 W/g. With the help of forced air cooling, temperature of vessel heating during the operation of the mill was kept not higher than 60 °C. The vessels, 45 ml in volume each, and the balls (20 sp., diameter: 10 mm) were made of ShKh15 steel (concentrations of C and Cr 1 and 1.5 mass %, respectively). The mass of the charged powder was 10 g for each given time of mechanical treatment. Possible contamination of the samples with the material of milling bodies due to wearing was monitored by measuring the mass of vessels, balls and the powder before and after treatment. Grinding time t_g was varied from 1 to 16 h. Investigations of the structural and phase state, chemical composition, shapes and sizes of the particles of ground powder were carried out with the help of X-ray diffraction (monochromatic CuK_α radiation),

Mossbauer spectroscopy (with ^{57}Fe nuclei) and Auger spectroscopy, secondary ion mass spectrometry (SIMS) and chemical analysis (CA). Measurement procedures and processing of the experimental results were described in detail elsewhere [10].

RESULTS AND DISCUSSION

No changes in the sample masses were observed during MA till the maximal grinding time (16 h). The secondary electron images of powder particles after mechanical treatment of the initial components for 1 and 16 h are shown in Fig. 1. The particles were disc-like with a thickness of 1–5 μm and mean diameter $\sim 80 \mu\text{m}$ after grinding for 1 h and lithoid with a mean diameter of $\sim 50 \mu\text{m}$ after grinding for 16 h. Layer by layer chemical analysis of the powder particles (SIMS) showed that the thickness of

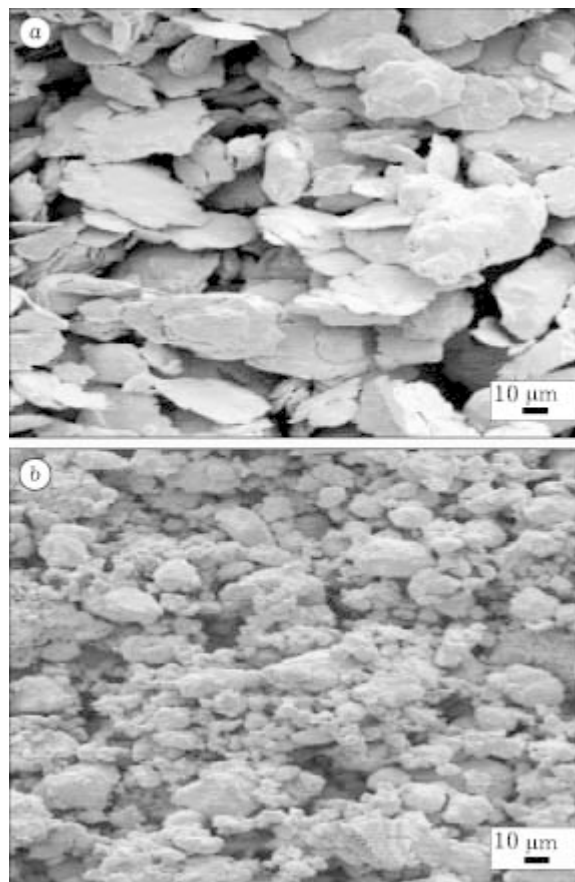


Fig. 1. Secondary electron images of powder particles after mechanical treatment of the initial components Fe and Mg for 1 (a) and 16 h (b).

TABLE 1

Chemical composition of the surface (SIMS) and volume (CA) of particles

t_g , h	Atomic concentration, %		Measuring procedure
	Fe	Mg	
1	71 ± 3	29 ± 2	SIMS
	94 ± 2	6.0 ± 0.5	CA
16	93 ± 3	7 ± 1	SIMS
	94 ± 2	6.0 ± 0.5	CA

the oxide layer on the surface of powder particles reaches 5–7 nm. The quantitative data on the chemical composition of particle surface (SIMS) and sample composition averaged over the entire volume (CA) are shown in Table 1. For the case of $t_g = 16$ h, the mean Mg content (CA) generally agrees with the initial composition of the mixture Fe(93)Mg(7). A similar situation is observed also for the surface layers of the sample in the case of the same grinding time. However, at an early stage of MA ($t_g = 1$ h) substantial enrichment of particles with magnesium is observed.

The regions of X-ray diffraction patterns in which we expected the most intensive reflections of the bcc Fe and HCP Mg to appear are shown in Fig. 2 for the early ($t_g = 30$ min) stage of MA. One can see that complete disappearance of the reflections of pure HCP Mg occurs as early as at $t_g = 30$ min when the new phases are not formed yet. Rapid disappearance of the reflections from Mg can be due to the absorption of X-rays by a fine mixture of Fe and Mg because the absorption factor of Mg for CuK_α radiation is much less than that of iron [11]. However, it should be noted that in mechanically alloyed immiscible system Fe(93)Bi(3) [12] rapid disappearance of the X-ray reflections of Bi (CuK_α radiation) was observed, without any indices of MA of Fe and Bi, though the absorption factors of the components were similar. The (211) reflections of α -phase and their approximation with the help of a doublet ($K_{\alpha 1}$, $K_{\alpha 2}$) of Voigt functions for longer grinding are shown in Fig. 3. One can see that the width of the reflection increases with an increase in grinding time; the reflection shifts to smaller 2θ angle region. The Mossbauer

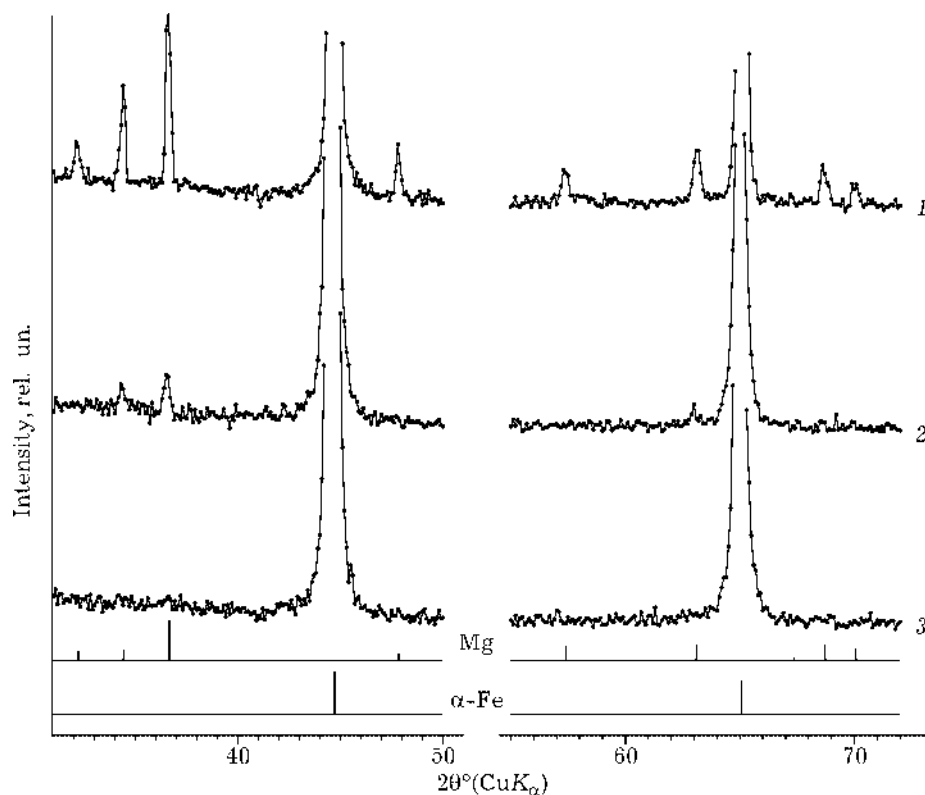


Fig. 2. The regions of X-ray diffraction patterns for the early stage of MA of the system Fe(93)Mg(7): 1 – initial sample, 2 – $t_g = 15$ min, 3 – $t_g = 30$ min.

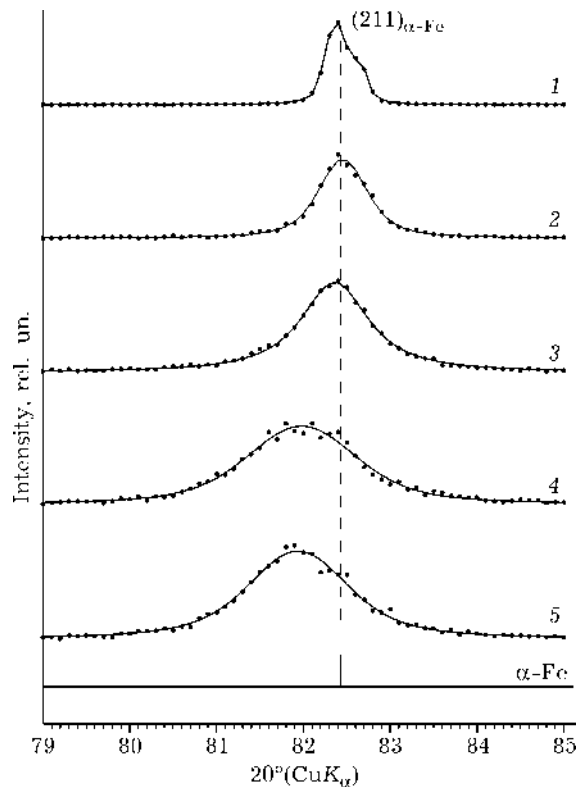


Fig. 3. The bcc (211) X-ray reflections after MA for different time in the system Fe(93)Mg(7): 1 – initial sample, 2 – $t_g = 1$ h, 3 – $t_g = 2$ h, 4 – $t_g = 5$ h, 5 – $t_g = 16$ h; continuous line is the approximation with Voigt functions.

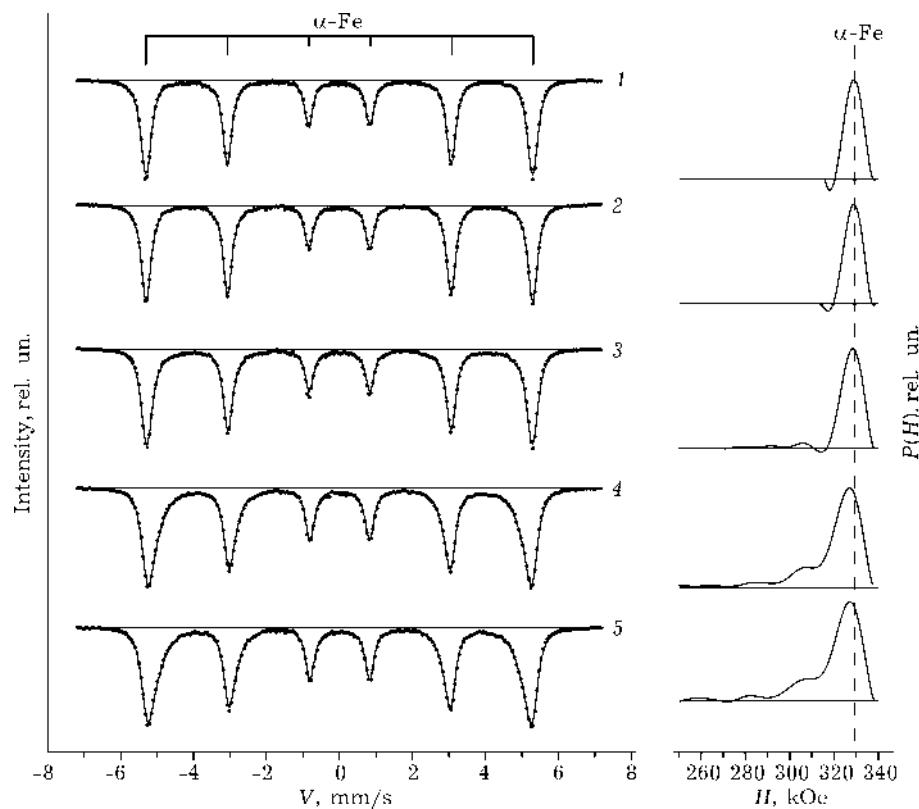


Fig. 4. Mossbauer spectra of the samples and the corresponding $P(H)$ functions depending on time of MA of the system Fe(93)Mg(7): 1 – initial, 2 – $t_g = 1$ h, 3 – $t_g = 2$ h, 4 – $t_g = 5$ h, 5 – $t_g = 16$ h.

spectra (Fig. 4) for $t_g \geq 2$ h exhibit the appearance of new components with smaller superfine magnetic field values (SPMF), which is the evidence of the appearance of Mg atoms in the closest surroundings of Fe atoms. The appearance of additional components is clearly seen in $P(H)$ functions. The shift of bcc reflections in the diffraction patterns and the appearance of additional components in Mossbauer spectra point to the formation of a SSS of Mg in α -Fe. Approximation of the reflections of bcc phase with a sole doubles ($K_{\alpha 1}$, $K_{\alpha 2}$) (see Fig. 3) allows us to assume that the dissolution of Mg in α -Fe occurs simultaneously over the whole grain volume. For comparison, the formation of a SSS of Si and Ge in α -Fe [3, 4, 6] is a heterogeneous process manifesting itself in the complicated structure of the (211) reflection which is composed of the contributions from pure α -Fe and the formed solid solution α -Fe (Si or Ge).

The results of quantitative analysis of the experimental data are shown in Fig. 5. All the structural phase changes in the system start at $t_g = 2$ h, when the size of α -Fe grain reaches

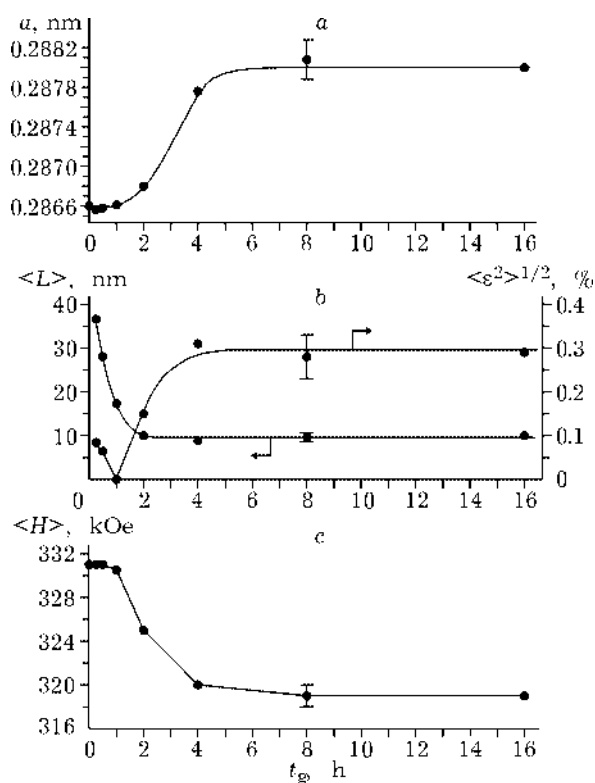


Fig. 5. Temporal dependencies of the bcc lattice parameter (a), mean grain size and the level of microdistortions of the bcc phase (b), and mean superfine field on Fe nuclei (c).

the nanometer size (~ 10 nm) (see Fig. 5, b). This is accompanied by a sharp increase in the lattice parameter of the bcc phase to 0.2880 nm (see Fig. 5, a) and by a decrease in the mean SFMF to 320 kOe at $t_g = 4$ h (see Fig. 5, c). Microdistortions start to grow at $t_g = 2$ h (see Fig. 5, b). So, there is an incubation period in the saturation of Fe with Mg; this period lasts for about 1 h. It paves the way for the formation of SSS, mainly due to the grinding of α -Fe grains. As we have mentioned earlier, this period is characterized by substantial enrichment of the particle surface with magnesium (see Table 1).

Magnesium, being much softer metal in comparison with iron ($HB_{Mg} = 300$ MPa, $HB_{Fe} = 800$ MPa), can be much easier deformed; at the initial stages of mechanical activation it can coat iron particles. In addition, it should be noted that the surface energy σ of magnesium is much less than that of iron (0.76 and 2.475 J/m², respectively) [13]; so, arrangement of magnesium over the surface of iron particles should decrease the contribution from the surface into the energy

of the system. The same effect for the energy of intergranular boundaries in iron should be expected in the case when Mg is distributed over the grain boundaries.

If we assume that all the magnesium is situated on the surface of Fe particles at the end of incubation period, then, taking into account the shape and size of powder particles (see Fig. 1 for $t_g = 1$ h), we obtain the layer thickness of approximately 130 nm. The surface magnesium can be detected by means of X-ray diffraction if the thickness of the layer to be analyzed is decreased by changing the recording geometry of the diffractometer. Figure 6 shows a part of the diffraction patterns for $t_g = 1$ h obtained under the conditions of symmetrical recording (Bragg–Brentano focusing) (see Fig. 6, a) with the layer under analysis ~ 3 μ m thick; for comparison, the patterns obtained in the sliding geometry with a fixed angle of incidence of the primary beam $\alpha = 1^\circ$ are shown (see Fig. 6, b). In the latter case, for CuK_α radiation, the depth of the layer under analysis was ~ 50 nm. One can see that in both cases no reflections of HCP Mg are

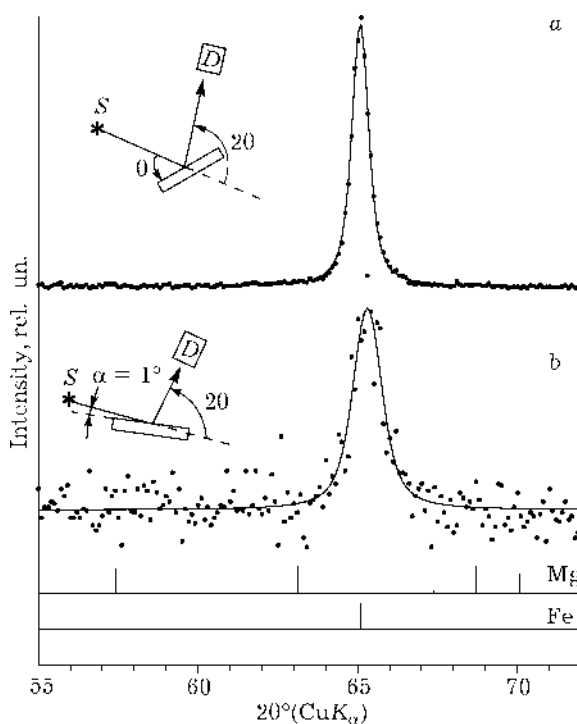


Fig. 6. Part of the X-ray diffraction patterns of Fe(93)Mg(7) system for $t_g = 1$ h, obtained under the conditions of symmetrical recording (a), and under the sliding geometry with a fixed angle of incidence of the primary rays $\alpha = 1^\circ$ (b).

detected. Hence, the major part of Mg is present in the particle volume.

The analysis of the data obtained in experiments allows assuming that MA in the system Fe–Mg starts from grinding the crystallites of components, segregation of Mg along the boundaries of α -Fe nanograins, and the formation of Fe/Mg nanocomposite. It was shown in [9] with the help of thermodynamic modeling that the driving force of the formation of SSS during MA in the system Fe–Mg can be the excess energy of the coherent interphase boundaries in the Fe/Mg nanocomposite. As the dispersity of the phase constituents Fe and Mg increases (particle size decreases), the boundaries between phases become coherent. Elastic distortions caused by misfit between the domains of Fe and Mg lattices relax in part due to the atomic rearrangement of HCP Mg with the formation of bcc structure. The accumulated energy of coherent boundaries of the nanocomposite can act as a thermodynamic stimulus for the formation of the SSS. Using the procedure described in [9] we obtain for the case of initial mixture Fe(93)Mg(7): enthalpy of the SSS ΔH_{SSS} and enthalpy of Fe/Mg nanocomposite ΔH_{comp} – 6 and 20 kJ/mol, respectively. The enthalpy of formation of the Fe/Mg nanocomposite is higher than that for the SSS; so, the formation of a solid solution from the nanocomposite is profitable from the point of view of thermodynamics.

Estimation of the lattice parameter for the SSS Fe + 7 at. % Mg with the help of Vegard rule gives 0.290 nm, which is much larger than the parameter determined experimentally (0.228 nm) for long-term grinding (see Fig. 5, a). The difference may be due to the fact that a part of magnesium does not form the solid solution but remains localized in the boundaries of nanograins as segregates.

CONCLUSIONS

Surface enrichment of iron powder particles with magnesium is observed at the initial stage

of MA of a mixture of pure Fe and Mg powders of the composition Fe(93)Mg(7). It is concluded that Mg gets segregated not only on the particle surface but also within the boundaries of α -Fe grains. Later on, when the crystallite size decreases to ~ 10 nm, supersaturated solid solution of Mg in α -Fe is formed, which is observed as an increase in the parameter of the bcc lattice (to 0.288 nm) and the appearance of additional components in M \ddot{u} ssbauer spectra. It was established on the basis of model calculations that the driving force of the formation of solid solution in the system Fe–Mg can be the accumulated excess energy of coherent interphase boundaries of Fe/Mg nanocomposite which is formed at the initial stage of MA.

Acknowledgement

The authors thank F. Z. Gilmutdinov and V. I. Ladyanov for carrying out determination of the chemical composition of the surface and volume of powder particles.

REFERENCES

- 1 E. P. Yelsukov, G. A. Dorofeev, V. A. Barinov *et al.*, *Mater. Sci. Forum*, 269–272 (1998) 151.
- 2 G. A. Dorofeev, E. P. Yelsukov, A. L. Ulyanov and G. N. Konygin, *Ibid.*, 343–346 (2000) 585.
- 3 G. A. Dorofeev, A. L. Ulyanov, G. N. Konygin, E. P. Yelsukov, *FMM*, 91, 1 (2001) 47.
- 4 E. P. Yelsukov, G. A. Dorofeev, G. N. Konygin *et al.*, *Ibid.*, 93, 3 (2002) 93.
- 5 E. P. Yelsukov, G. A. Dorofeev, V. M. Fomin *et al.*, *Ibid.*, 94, 4 (2002) 43.
- 6 E. P. Yelsukov, G. A. Dorofeev, A. L. Ulyanov *et al.*, *Ibid.*, 95, 2 (2003) 60.
- 7 O. Kubashevski, *Diagrammy sostoyaniya dvoynykh sistem na osnove zheleza*, Metallurgiya, Moscow, 1985.
- 8 A. Hightower, B. Fultz and R. C. Bowman, *J. Alloys Compd.*, 252 (1997) 238.
- 9 G. A. Dorofeev, E. P. Yelsukov, A. L. Ulyanov, *Neorg. Mat.*, 40 (2004) 793.
- 10 E. P. Yelsukov, G. A. Dorofeev, A. L. Ulyanov, A. V. Zagaynov, *FMM*, 95 (2003) 88.
- 11 R. T. Leonard and C. C. Koch, *Scripta Mater.*, 36 (1997) 41.
- 12 N. Lyakhov, T. Grigorieva, A. Barinova *et al.*, *J. Mater. Sci.*, 39 (2004) 5421.
- 13 H. Bakker, *Mater. Sci. Found.*, 1–1 (1998) 1.